RAPID REPORT

HUMAN FEAR-RELATED MOTOR NEUROCIRCUITRY

T. BUTLER,[a]* H. PAN,[a] O. TUESCHER,[a]
A. ENGELIEN,[b] M. GOLDSTEIN,[a] J. EPSTEIN,[a]
D. WEISHOLTZ,[a] J. C. ROOT,[a] X. PROTOPOPESCU,[a]
A. C. CUNNINGHAM-BUSSEL,[a] L. CHANG,[a] X.-H. XIE,[a]
Q. CHEN,[a] E. A. PHELPS,[c] J. E. LEDOUX,[d] E. STERN[a]
AND D. A. SILBERSWEIG[a]

[a]*Functional Neuroimaging Laboratory, Department of Psychiatry, Weill Medical College of Cornell University, Box 140, 1300 York Avenue, New York, NY 10021, USA*

[b]*Department of Psychiatry and Interdisciplinary Center for Clinical Research, University of Muenster, Muenster, Germany*

[c]*New York University, Department of Psychology, New York, NY, USA*

[d]*New York University, Center for Neural Science, New York, NY, USA*

Abstract—Using functional magnetic resonance imaging and an experimental paradigm of instructed fear, we observed a striking pattern of decreased activity in primary motor cortex with increased activity in dorsal basal ganglia during anticipation of aversive electrodermal stimulation in 42 healthy participants. We interpret this pattern of activity in motor neurocircuitry in response to cognitively-induced fear in relation to evolutionarily-conserved responses to threat that may be relevant to understanding normal and pathological fear in humans. © 2007 IBRO. Published by Elsevier Ltd. All rights reserved.

Key words: fMRI, anxiety, freezing, basal ganglia, motor cortex, amygdala.

Advances in our understanding of fear-related neurocircuitry have depended critically upon the ability to assess fear in laboratory animals through measurement of motor phenomena such as fear-induced freezing and fear-potentiated startle (LeDoux, 2000). Yet fear-related motor phenomena in humans have received much less attention, perhaps because unlike animals, humans are conscious of their fears, and can describe and quantify them verbally. But such high-level, uniquely human fear responses have not *replaced* more primitive ones; healthy humans still become "scared stiff" and "jump out of their skin" just like laboratory animals (Blanchard et al., 2001). Using a translationally-derived functional magnetic resonance imaging (fMRI) paradigm of instructed fear/anticipatory anxiety (Phelps et al., 2001), we demonstrate that brain regions traditionally considered to be involved mainly in motor behavior (primary motor cortex and dorsal basal ganglia) actually respond robustly to an experimentally-induced state of conscious fear.

EXPERIMENTAL PROCEDURES

Participants

Forty-two healthy, right-handed participants (mean age: 28 [std 6]; 16 women) underwent fMRI scanning as part of this study, which was approved by the Weill-Cornell Institutional Review Board.

Dial-up procedure

Immediately prior to scanning, each participant determined the level of electrodermal stimulation to be received during the scan session via a standardized dial-up procedure in which stimulations to the left wrist were increased gradually to a level of intensity experienced by that individual as "uncomfortable but not painful," with the aim of standardizing perceived stimulation aversiveness across subjects. Following the dial-up procedure, participants were told "all stimulations you receive during this study will be of exactly this strength and duration."

Experimental paradigm

The scanning session consisted of a "threat" condition, about which participants were told "an electrodermal stimulation can occur at any time" and a "safety" condition during which participants knew they would receive no stimulations. Threat and safety were signified by the presentation of easily-distinguishable colored squares via an MR-compatible screen. Presentation of stimuli was controlled by the Integrated Functional Imaging System (*In vivo*, Orlando, FL, USA) by means of Eprime software (Psychology Software Tools, Pittsburgh, PA, USA). Pairing of colors with conditions was counterbalanced across participants. Each color appeared for a period of 12 s followed by an 18 s rest period. There were five pseudo-randomly ordered periods of each color per scanning run, and two scanning runs per study session (total of 10 12-s periods of each condition per study session). This paradigm required no motor response. Participants did not actually receive any electrodermal stimulations during scanning.

Skin conductance response (SCR)

Skin conductance was recorded during fMRI scanning to provide an independent physiological measure of arousal. Due to technical difficulties, SCR was recorded successfully only in later-scanned participants ($n=21$). SCR was acquired using electrodes attached to the distal phalanges of the second and third digits of the left hand (BIOPAC Systems, Santa Barbara, CA, USA). Shielded electrode leads were tightly twisted and extended from the magnet room through the penetration board into the control room, where the signal was amplified and recorded with a BIOPAC Systems skin conductance module connected to a laptop computer running AcqKnowledge software (BIOPAC Systems).

*Corresponding author. Tel: +1-212-746-3766; fax: +1-212-746-5818.
E-mail address: tab2006@med.cornell.edu (T. Butler).
Abbreviations: BOLD, blood oxygen level–dependent; fMRI, functional magnetic resonance imaging; ROI, region of interest; SCR, skin conductance response.

Data were recorded continuously at a rate of 200 samples per second. Off-line analysis of SCR waveforms was performed using Matlab 7 (MathWorks, Natick, MA, USA). Data were first smoothed using a sliding window average (window width=401 samples) and then subjected to a local peak-detection algorithm. Stimulus-related SCRs were defined as trough-to-peak conductance differences greater than 0.02 μS occurring within a window of 0.5 s to 12 s following stimulus onset. The amplitude of the largest SCR associated with each stimulus (SCR magnitude) was used as an index of the subject's maximum arousal during that stimulus (if no SCR was detected, amplitude was considered to be 0) (Dawson et al., 2000). The distribution of these maximum SCRs was normalized (log [SCR+1]), then averaged within the threat and the safety conditions for each subject. Paired two-tailed t-test was used to assess differences in mean SCR magnitude between threat and safety.

Debriefing

Immediately following scanning, participants' subjective level of fear/anxiety was assessed using a scripted debriefing questionnaire.

Image acquisition and processing

Gradient echoplanar functional images (TR=1200; TE=30; flip angle=70°; FOV=240 cm; 15 5 mm slices; 1 mm interslice space; matrix=64×64) sensitive to blood oxygen level–dependent (BOLD) signal were obtained on one of two GE-Signa 3T MRI scanners (GE Healthcare, Waukesha, WI, USA). Scanner 1 was used from 2001 to 2003; scanner 2 was used from 2003 to 2006. Twenty-three participants were scanned on scanner 1; 19 on scanner 2. Because there were no detectable differences in imaging data acquired on the two scanners, datasets were combined. Images were acquired using a modified z-shimming algorithm to minimize susceptibility artifact at the base of the brain (Gu et al., 2002). A reference T1-weighted anatomical image with the same axial slice placement and thickness as the functional imaging was acquired to aid reorientation and coregistration. A high-resolution T1-weighted anatomical image was acquired using a spoiled gradient recalled acquisition sequence (TR/TE=30/8 ms, flip angle=45, FOV=240 mm, 100 1.5 mm axial slices; matrix=256×256). Functional image processing consisted of the following steps using customized SPM software (http://www.fil.ion.ucl.ac.uk/spm): Reconstruction of functional images using modified GE reconstruction software with off-resonance phase correction, slice-timing correction and Hanning-window apodization; manual AC-PC reorientation of all anatomical and functional images; realignment to correct for slight head movement between scans and for differential spin excitation history based on intracranial voxels (datasets with movement of greater than 1/3 voxel over the duration of the study session were excluded); extraction of physiological fluctuations such as cardiac and respiratory cycles from functional image sequence; co-registration of functional images to the corresponding high-resolution anatomical image based on the rigid body transformation parameters of the reference anatomical image to the latter for each individual participant; stereotactic normalization (to Montreal Neurological Institute space) based on the high-resolution anatomical image; spatial smoothing with an isotropic Gaussian kernel (FWHM=7.5 mm) to increase signal-to-noise ratio.

Image analysis

For functional image analysis, a two-stage voxel-wise linear mixed-effects model was used (Worsley et al., 2002). First, a voxel-by-voxel univariate multiple linear regression model at the participant level determined the extent to which each voxel's activity correlated with the principal regressors, which consisted of onset times and durations of threat and safety periods convolved with a prototypical hemodynamic response function. The first order temporal derivatives of the principal regressors, temporal global fluctuation, physiological fluctuations, realignment parameters, and scanning periods were incorporated as covariates of no interest. Temporal high-pass filtering was performed with a set of polynomial basis functions to counter the effects of baseline shift, and a voxel-wise *AR(1)* model of the time course accommodated temporal correlation in consecutive scans. This first level analysis resulted in a set of participant- and condition-specific effect images and corresponding standard deviation images, which were combined in a series of linear contrasts and entered into a second-level analysis to assess the group effect sizes. A mixed-effects model with the participant factor as the random effect, and six nuisance covariates [age, sex, scanner, safe color, experiment order and type (before or after one of two separate verbal experiments)] was employed to account for inter- and intra-participant variability and allow population-based inferences to be drawn. Results were considered significant if they survived family-wise error correction for multiple comparisons over the whole brain at $P<0.05$.

Image analysis: region of interest (ROI) approach

Given a priori interest in the amygdala based on animal studies of fear conditioning (LeDoux, 2000), results in this region were assessed using a standard bilateral anatomical mask (Tzourio-Mazoyer et al., 2002), and were considered significant if they survived small volume correction at $P<0.05$.

RESULTS

SCR and debriefing questionnaire

Analysis of 14 skin conductance tracings (seven traces [out of 21] could not be analyzed due to excessive artifact or no detectable SCRs) revealed significantly larger SCR
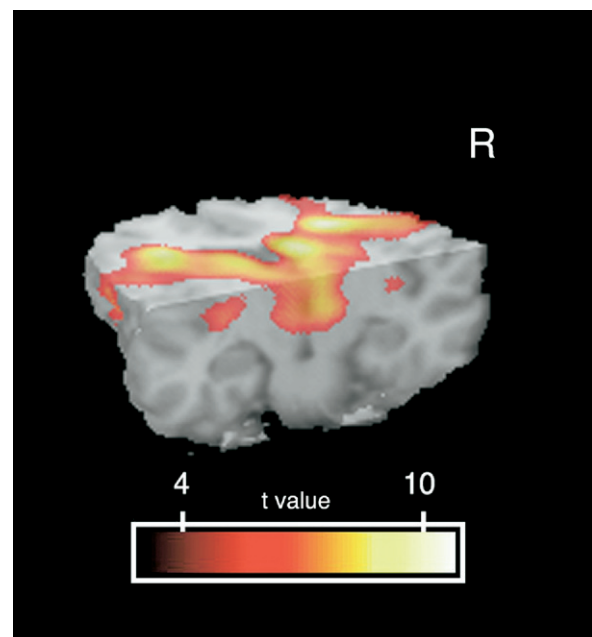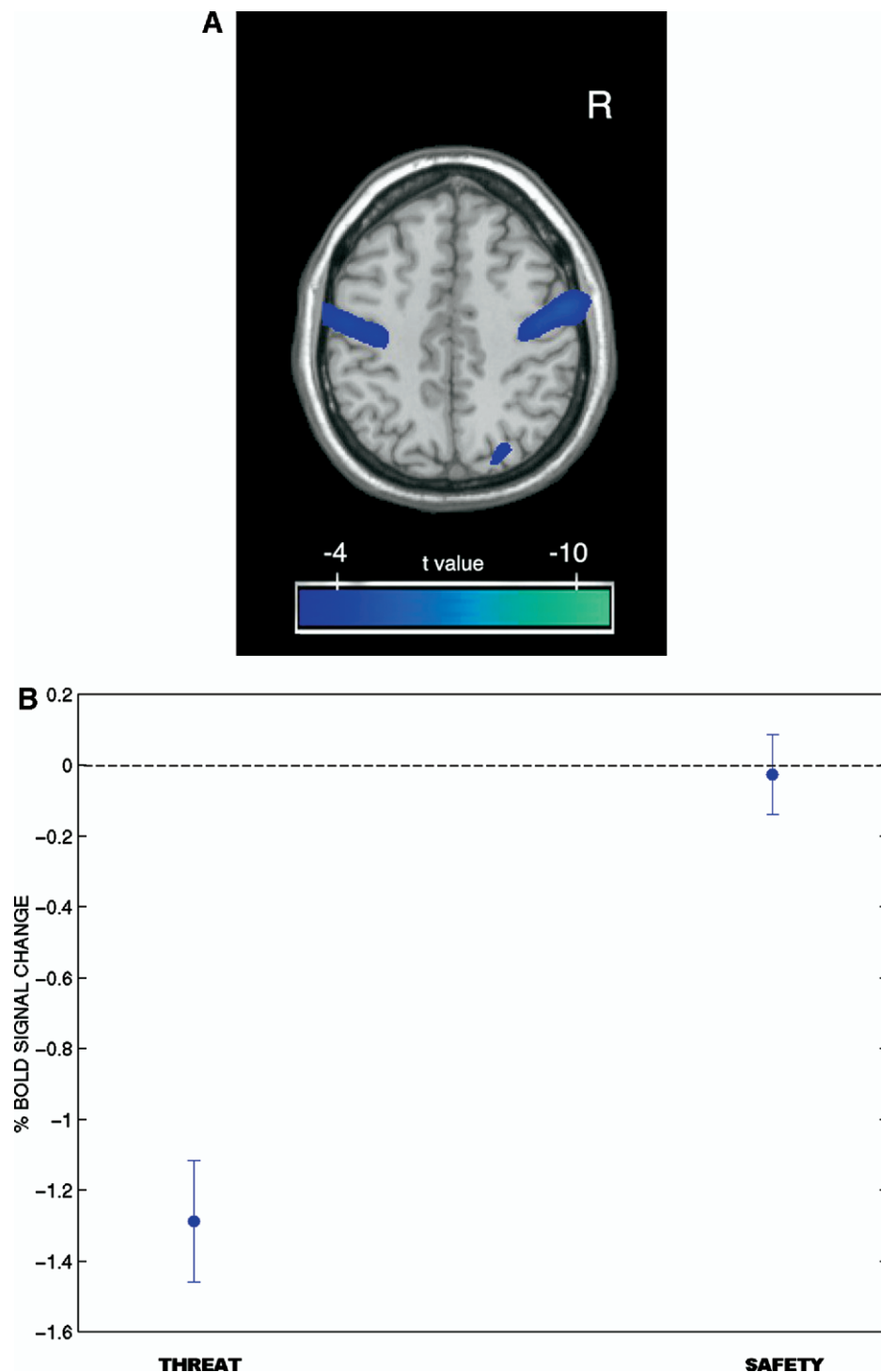

Fig. 1. Increased activity in bilateral insula, dorsal basal ganglia and thalamus (extending down to hypothalamus and midbrain) during threat as compared with safety [$P_{unc}<.001$; viewed from left posterior perspective at axial plane z=10 mm, coronal plane y=−18 mm].

magnitudes during threat as compared with safety, $t(13)=3.23$, $P=0.007$ (two-tailed), Cohen's $d=1.07$.

Responses to the post-scan debriefing question "How did you feel when seeing each of the two colors?" were available for 38/42 participants. Thirty-three of 38 partici-

pants (86.8%) reported feeling anxious or fearful about receiving a shock during the threat condition. Three participants (7.9%) stated they were not anxious during the threat condition, while the responses of two participants could not be coded as anxious or non-anxious.

Fig. 2. (A) Decreased activity in bilateral motor cortex during threat as compared with safety [$P_{unc}<.001$; axial plane $z=45$ mm]. (B) Plot with standard deviation bars showing condition-specific activity at peak right primary motor cortex voxel ($x=48$, $y=-9$, $z=39$). Note right motor cortex suppression during threat as compared with safety, and relative to a resting baseline (indicated by dotted line). Pattern of activity in left motor cortex was similar.

fMRI results: whole-brain

During threat as compared with safety, there was increased activity in bilateral dorsal basal ganglia (peak activation in right caudate: $x=12$, $y=12$, $z=9$; z score >8, $P_{corr}<.001$; shown in Fig. 1), as well as in bilateral anterior insula, right dorsolateral prefrontal cortex, dorsal anterior cingulate and bilateral thalamus extending down to hypothalamus and midbrain.

There was *decreased* activity during threat as compared with safety (and as compared with a resting baseline) in bilateral primary motor cortex (left: $x=-45$, $y=-12$, $z=36$; z score $=-5.49$, $P_{corr}<.001$; right: $x=48$, $y=-9$, $z=39$; z score $=-5.83$, $P_{corr}<.001$; shown in Fig. 2), as well as in bilateral hippocampi/parahippocampi, posterior cingulate/precuneus, and angular gyri.

Results are listed in Table 1.

fMRI results: amygdala ROI

There was no overall difference in amygdalar activity during threat as compared with safety ($P_{corr}>.1$). In other words, when average activity during the 10 threat periods was compared with average activity during the 10 safety periods, no condition-specific amygdalar activity was detected. However, because fear-related amygdalar activity is known to habituate over time (Zald, 2003), amygdalar activity was examined separately for each of the 10 threat

periods (five in each of two scanning runs) to assess possible changes over the course of the experiment. As shown in Fig. 3A, increased activity in left amygdala/extended amygdala was present *only* during the very first threat period ($x=-15$, $y=-3$, $z=-12$; Z-score$=3.73$; $P_{corr}=.015$). As shown in Fig. 3B, there was some degree of bilateral amygdalar activity during this first threat period, though right amygdala findings did not attain statistical significance ($x=18$, $y=0$, $z=-15$; Z-score$=3.14$; $P_{corr}=.084$).

All the abovementioned fMRI results were similar when the analysis included only participants for whom SCR data were available ($n=14$). A subsequent step-wise regression analysis of the BOLD effects of the 42 subjects with SCR presence/absence factor as a covariate of no interest at the brain regions of the key findings showed that virtually no portion of the total variance was explained by the SCR factor ($P>0.1$).

DISCUSSION

Results indicate that brain regions traditionally considered to be involved mainly in motor behavior (dorsal basal ganglia and primary motor cortex) respond robustly and consistently to an experimentally-induced state of conscious fear, while threat-related amygdalar activity is limited to the earliest portion of the experiment. Actual movement is an

Table 1. Brain regions showing significantly increased or decreased activity during threat as compared to safety

Z score	P_{corr}	x	y	z	Region
Increased: threat vs. safety					
>8	<0.001	12	12	9	R caudate
>8	<0.001	33	27	9	R anterior insula/inferior frontal
>8	<0.001	−30	27	9	L anterior insula/inferior frontal
7.296	<0.001	−15	6	9	L putamen
7.209	<0.001	48	21	−3	R anterior insula/inferior frontal
7.205	<0.001	21	6	0	R putamen
6.667	<0.001	6	−18	9	R thalamus (peak in medial dorsal nucleus)
6.198	<0.001	−9	−9	6	L thalamus (peak in ventrolateral nucleus)
5.93	<0.001	3	30	39	b/l Dorsal anterior cingulate/medial prefrontal cortex
5.709	<0.001	51	−33	36	R inferior parietal lobule (BA 40)
5.582	<0.001	−69	−24	30	L inferior parietal lobule (BA 40)
5.253	<0.001	39	9	39	R dorsolateral prefrontal cortex (DLPFC, BA9)
5.25	<0.001	−57	15	3	L inferior frontal gyrus (BA 45)
5.232	<0.001	0	−30	30	b/l Dorsal cingulate/posterior cingulate
5.16	0.01	27	−99	−6	R occipital (cuneus)
4.93	0.02	48	18	27	R DLPFC (BA46)
4.678	0.05	−30	−21	3	L putamen
Decreased: threat vs safety					
7.004	<0.001	−39	−12	21	L precentral gyrus
6.883	<0.001	45	−66	33	R angular gyrus
6.583	<0.001	−27	−18	−15	L hippocampus/parahippocampus
6.461	<0.001	12	−48	3	Posterior cingulate/precuneus
5.827	<0.001	48	−9	39	R precentral gyrus (primary motor cortex)
5.755	<0.001	30	−15	−18	R hippocampus/parahippocampus
5.729	<0.001	−3	75	3	L rostral superior frontal gyrus
5.485	<0.001	−45	−12	36	L precentral gyrus (primary motor cortex)
4.859	0.03	−12	−81	30	L occipital (BA19)
4.726	0.04	−42	−66	39	L parietal (close to angular gyrus)

Peaks listed survived family-wise error correction for multiple comparisons over the whole brain ($P_{corr}<0.05$).
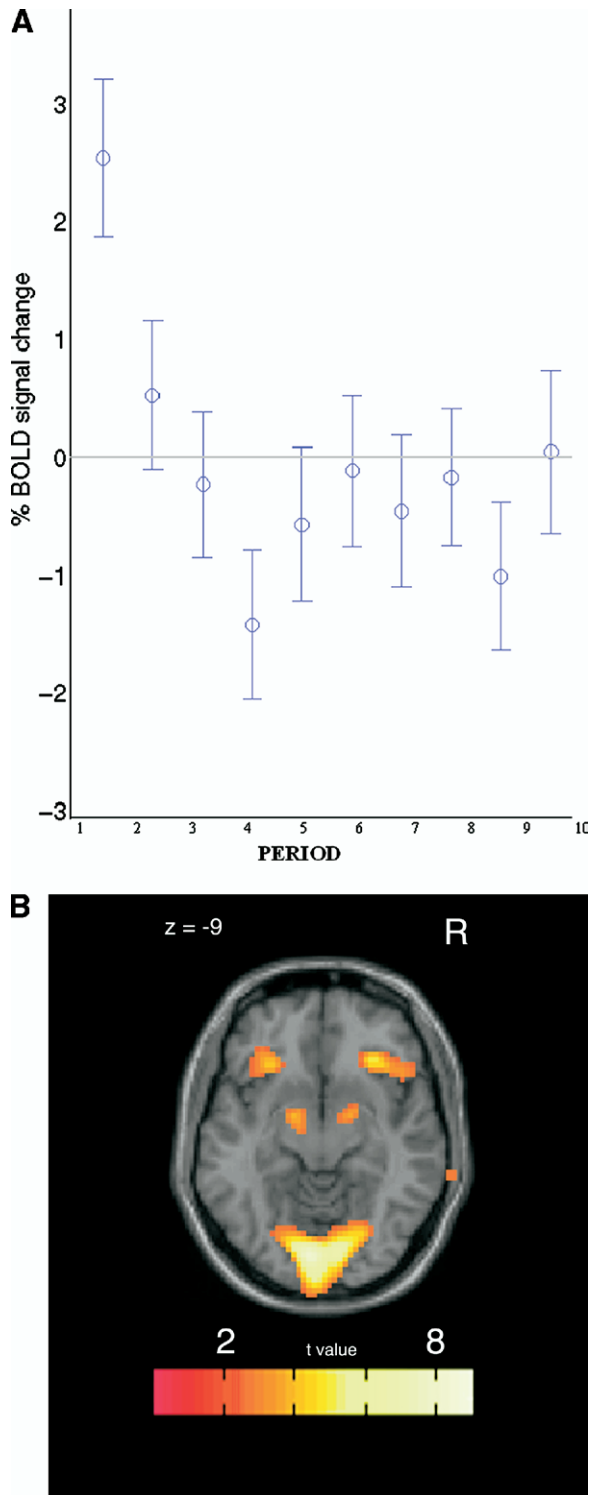
Fig. 3. (A) Plot with standard deviation bars showing activity in peak left amygdala voxel (x=−15, y=−3, z=−12) during each of 10 12-s periods of threat. Note that left amygdala activity was elevated above a resting baseline only during the very first period of threat. (B) Increased bilateral (L>R) amygdala/extended amygdala activity during first (of 10) periods of threat (as compared with rest; results were similar when compared with safety). For illustration purposes, image is displayed at threshold of $P_{unc} < .01$. Threat-related activity in bilateral anterior insula and primary visual cortex is also apparent.

unlikely explanation for findings because no experimental condition required any motor response. That the experimental paradigm produced fear/anxiety in participants as intended is supported by physiological (SCR) and behavioral (debriefing) data.

Basal ganglia and motor cortex

Increased threat-related basal ganglia activity may be understood as representing a state of motor readiness in response to danger. Dorsal basal ganglia activation has been noted in prior functional imaging studies of normal (Phelps et al., 2001) and pathological (Rauch et al., 1994, Lorberbaum et al., 2004) human fear. The basal ganglia are a critical emotion/motor interface that allow an organism to translate emotional information into behavioral responses (Ring and Serra-Mestres, 2002, Grillner et al., 2005). Present results indicate that cognitively-based fear engages motor control networks, including cortico-striato–thalamic loops (Alexander et al., 1986) involved in preparatory set and in determining and executing situationally-appropriate action. In particular, activation of caudate, putamen, thalamus, dorsolateral prefrontal cortex and dorsal anterior cingulate suggests involvement of both executive and motor circuits.

In association with increased activity in basal ganglia, striking motor cortex de-activation was seen during threat. At least one prior study (Boshuisen et al., 2002) detected very similar findings of motor cortex hypoperfusion during anticipatory anxiety (in patients with panic disorder), though other studies employing similar experimental paradigms have tended not to report areas of decreased activity during anticipation of aversive stimulation (Chua et al., 1999, Ploghaus et al., 1999, Phelps et al., 2001), and/or have focused exclusively on regions of predefined interest which have not included motor cortex (Porro et al., 2002, Nitschke et al., 2006).

The detected pattern of motor cortex de-activation and subcortical (basal ganglia, thalamus, brainstem) activation during threat can in a general sense be interpreted as reflecting a shift from cortical to subcortical processing during danger. This interpretation fits with animal studies showing that cortical structures are not critical for responding appropriately to danger, and that fight or flight motor programs are mediated predominantly by evolutionarily-conserved subcortical structures, with basal ganglia playing a critical role (Grillner et al., 2005).

We speculate that present findings of threat-related activity in motor regions may be relevant to understanding several motor phenomena associated with human fear or anxiety. These phenomena range from voluntary or semi-voluntary "top down" tensing of muscles to prepare for consciously-anticipated discomfort and/or to avoid flinching, a presumably uniquely human phenomenon mentioned as a possible explanation for findings in motor regions in prior functional neuroimaging studies of fear (Phelps et al., 2001, Boshuisen et al., 2002), to more automatic and likely evolutionarily-based "bottom up" fear-related motor processes such as fear-potentiated startle (Grillon and Baas, 2003), fear-related loss of manual dex-

terity (Noteboom et al., 2001), and fear-induced freezing, which is known to occur in healthy humans in dangerous situations (Blanchard et al., 2001), and which has been posited to be a feature of several neuropsychiatric disorders (Northoff, 2002, Moskowitz, 2004, Bystritsky et al., 2000, Cortese and Uhde, 2006, Lieberman, 2006). Additional work is needed to translate extensive knowledge of motor fear responses and underlying neurocircuitry in laboratory animals to understanding analogous normal and pathological motor fear responses in humans.

Limitations concerning motor interpretation of this study include absence of electromyography or other means for assessing possible subtle participant movement or changes in muscle tone.

Amygdala

In contrast to sustained threat-related increased activity in basal ganglia, insula, thalamus and brainstem, amygdalar activity (left>right) was present only during the earliest period of threat. This finding is broadly consistent with the previous publication on instructed fear (Phelps et al., 2001), and supports a model of the amygdala as an easily-habituable threat and novelty detector (Zald, 2003) whose early, brief, phasic activity in response to danger is accompanied by sustained tonic activity in brain regions responsible for maintaining vigilance, autonomic, metabolic and motor readiness for as long as danger persists.

Hippocampus

The unexpected finding of prominent hippocampal deactivation during threat, also reported in a previous study (Javanmard et al., 1999), may relate to intense focus on the future under conditions of imminent threat, with temporary suspension of a normal, "default" mode of evaluative processing (Raichle et al., 2001) including replay of past experiences. In support of this notion, apart from motor cortex, most of the regions found to be less active during threat as compared with safety (hippocampi, posterior cingulate, angular gyri) are considered key components of the default network.

CONCLUSION

The role of cortical and subcortical neurocircuitry in evolutionarily-conserved motor and other responses to perceived danger deserves additional translational study in animals models, in healthy humans, and in patients suffering from fear-related disorders.

REFERENCES

Alexander GE, DeLong MR, Strick PL (1986) Parallel organization of functionally segregated circuits linking basal ganglia and cortex. Annu Rev Neurosci 9:357–381.

Blanchard DC, Hynd AL, Minke KA, Minemoto T, Blanchard RJ (2001) Human defensive behaviors to threat scenarios show parallels to fear- and anxiety-related defense patterns of non-human mammals. Neurosci Biobehav Rev 25:761–770.

Boshuisen ML, Ter Horst GJ, Paans AM, Reinders AA, den Boer JA (2002) rCBF differences between panic disorder patients and control subjects during anticipatory anxiety and rest. Biol Psychiatry 52:126–135.

Bystritsky AA, Craske MM, Maidenberg EE, Vapnik TT, Shapiro DD (2000) Autonomic reactivity of panic patients during a CO2 inhalation procedure. Depression and anxiety 11:15–26.

Chua P, Krams M, Toni I, Passingham R, Dolan R (1999) A functional anatomy of anticipatory anxiety. Neuroimage 9:563–571.

Cortese BM, Uhde TW (2006) Immobilization panic. Am J Psychiatry 163:1453–1454.

Dawson M, Schell A, Fillon D (2000) The electrodermal system. In: Handbook of psychophysiology, 2nd ed (Cacioppo J, ed), pp 200–223. New York: Cambridge University Press.

Grillner S, Hellgren J, Menard A, Saitoh K, Wikstrom MA (2005) Mechanisms for selection of basic motor programs: roles for the striatum and pallidum. Trends Neurosci 28:364–370.

Grillon C, Baas J (2003) A review of the modulation of the startle reflex by affective states and its application in psychiatry. Clin Neurophysiol 114:1557–1579.

Gu H, Feng H, Zhan W, Xu S, Silbersweig DA, Stern E, Yang Y (2002) Single-shot interleaved z-shim EPI with optimized compensation for signal losses due to susceptibility-induced field inhomogeneity at 3 T. Neuroimage 17:1358–1364.

Javanmard M, Shlik J, Kennedy SH, Vaccarino FJ, Houle S, Bradwejn J (1999) Neuroanatomic correlates of CCK-4-induced panic attacks in healthy humans: a comparison of two time points. Biol Psychiatry 45:872–882.

LeDoux JE (2000) Emotion circuits in the brain. Annu Rev Neurosci 23:155–184.

Lieberman A (2006) Are freezing of gait (FOG) and panic related? J Neurol Sci 248:219–222.

Lorberbaum JP, Kose S, Johnson MR, Arana GW, Sullivan LK, Hamner MB, Ballenger JC, Lydiard RB, Brodrick PS, Bohning DE, George MS (2004) Neural correlates of speech anticipatory anxiety in generalized social phobia. Neuroreport 15:2701–2705.

Moskowitz AK (2004) "Scared stiff": catatonia as an evolutionary-based fear response. Psychol Rev 111:984–1002.

Nitschke JBJB, Sarinopoulos II, Mackiewicz KLKL, Schaefer HSHS, Davidson RJRJ (2006) Functional neuroanatomy of aversion and its anticipation. Neuroimage 29:106–116.

Northoff G (2002) Catatonia and neuroleptic malignant syndrome: psychopathology and pathophysiology. J Neural Transm 109:1453–1467.

Noteboom JT, Fleshner M, Enoka RM (2001) Activation of the arousal response can impair performance on a simple motor task. J Appl Physiol 91:821–831.

Phelps EA, O'Connor KJ, Gatenby JC, Gore JC, Grillon C, Davis M (2001) Activation of the left amygdala to a cognitive representation of fear. Nat Neurosci 4:437–441.

Ploghaus A, Tracey I, Gati JS, Clare S, Menon RS, Matthews PM, Rawlins JN (1999) Dissociating pain from its anticipation in the human brain. Science 284:1979–1981.

Porro CA, Baraldi P, Pagnoni G, Serafini M, Facchin P, Maieron M, Nichelli P (2002) Does anticipation of pain affect cortical nociceptive systems? J Neurosci 22:3206–3214.

Raichle ME, MacLeod AM, Snyder AZ, Powers WJ, Gusnard DA, Shulman GL (2001) A default mode of brain function. Proc Natl Acad Sci U S A 98:676–682.

Rauch SL, Jenike MA, Alpert NM, Baer L, Breiter HC, Savage CR, Fischman AJ (1994) Regional cerebral blood flow measured during symptom provocation in obsessive-compulsive disorder using ox-

ygen 15-labeled carbon dioxide and positron emission tomography. Arch Gen Psychiatry 51:62–70.

Ring HA, Serra-Mestres J (2002) Neuropsychiatry of the basal ganglia. J Neurol Neurosurg Psychiatry 72:12–21.

Tzourio-Mazoyer N, Landeau B, Papathanassiou D, Crivello F, Etard O, Delcroix N, Mazoyer B, Joliot M (2002) Automated anatomical labeling of activations in SPM using a macroscopic anatomical parcellation of the MNI MRI single-subject brain. Neuroimage 15:273–289.

Worsley KJ, Liao CH, Aston J, Petre V, Duncan GH, Morales F, Evans AC (2002) A general statistical analysis for fMRI data. Neuroimage 15:1–15.

Zald DH (2003) The human amygdala and the emotional evaluation of sensory stimuli. Brain Res Brain Res Rev 41:88–123.